Kinetics and Mechanism of the Demetallation of Macrocyclic Nickel(II) Complexes by Cyanide

by **Liselotte Siegfried** and **Thomas A. Kaden***

Department of Chemistry, Spitalstrasse 51, CH-4004 Basel

Dedicated to Professor *André E. Merbach* on the occasion of his 65th birthday

The kinetics and the mechanism of the cyanide-induced demetallation of a series of Ni^{2+} complexes with macrocyclic ligands of different ring size (12- to 14-membered; see **1**–**4**) and steric constraints was studied. Although the rates differ by almost five orders of magnitude when compared to each other under fixed experimental conditions (pH 10.5, $[CN^-] = 10^{-2}$ M), all reactions proceed through the relatively rapid formation of cyano adducts $[Ni(CN)_nL]$ ($n = 1, 2$), which then react with additional CN^- or HCN to give the final products. Of paramount importance for the reaction rate is the geometry and configuration of the cyano adducts $[Ni(CN)_nL]$ ($n = 1,2$). *cis*-Dicyano derivatives with a folded macrocycle react faster than *trans*-compounds. In the case of (1,4,8,11-tetraazacyclotetradecane)nickel(2+) ($[Ni(\mathbf{4})]^{2+}$), which gives a *trans*- dicyano adduct, the base-catalyzed N-inversion necessary to obtain the *cis*-dicyano derivative becomes rate determining at high CN^- concentrations.

Introduction. – The drastic differences in thermodynamic stability and kinetic inertness of open-chain tetramines and the corresponding tetraazamacrocyclic complexes are well documented in the literature (see, *e.g.*, [1]). So the high stability of the Cu^{2+} and Ni^{2+} complexes with the 14-membered cyclic tetramine **4** as compared to those of the analogous complexes with an open-chain tetramine ligand has been called the 'macrocyclic effect' [2][3]. This enhanced stability is almost entirely due to a more-favorable enthalpy. This results from the decreased ligand solvation of the macrocycle, which has less H-bonded H_2O to be displaced in the complex-formation process [3][4].

From the kinetic point of view, many macrocyclic complexes are extremely resistant against acid dissociation [5]. So the Cu^{2+} and Ni^{2+} complexes of 1,4,8,11-tetraazacyclotetradecane (**4**) do not dissociate in boiling dilute mineral acid, and their redox potential can easily be measured in 10M perchloric acid [6], conditions under which analogous complexes with open-chain ligands immediately dissociate. The inertness results from the fact that, in a macrocyclic metal complex, it is not possible to dissociate and protonate one amino group after the other in a stepwise process, but it is necessary to dissociate two amino groups of the macrocycle at the same time, a process that has a much higher activation energy than a stepwise dissociation.

In contrast, cyanide ions are able to decompose macrocyclic Ni^{2+} complexes. The reaction is driven on one side by the extremely high thermodynamic stability of $[Ni(CN)_4]^{2-}$ [7] and on the other side by the fact that the nucleophilic attack takes place at the Ni^{2+} center. This reaction has often been used for preparative purposes to destroy Ni^{2+} complexes of macrocycles, which were synthesized by template reactions [8]. In a few instances, it was shown that cyano adducts of the macrocyclic Ni^{2+} complexes are formed before the rate-determining step of the demetallation takes place [4][9].

Since little is known about the mechanism of this reaction, we present here a detailed and broad study of CN^--induced demetallation of a series of Ni^{2+} complexes with macrocycles **1**–**4** of different ring size and steric constraints and, therefore, different coordination geometries of the metal ion.

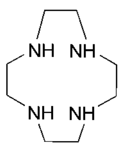

1

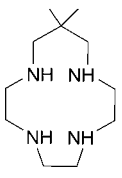

2

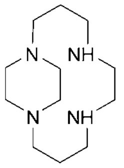

3

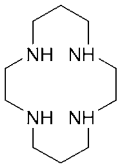

4

Results. – *Nickel(II) Complex of 1,4,7,10-Tetraazacyclododecane* (**1**). The CN^- dependencies of the demetallation of the Ni^{2+} complex with **1** show a square dependency on $[CN^-]$ at low cyanide concentration and a linear dependency at high cyanide concentration (*Fig. 1,b*). So, at least two CN^- ions must be involved in the rate-determining step. Measurements at higher complex concentrations at which the VIS bands of the Ni^{2+} chromophore can be detected indicate that, after mixing $[Ni(\mathbf{1})]^{2+}$ with CN^-, a new species with λ_{max} 510 and 780 nm is formed [9]. According to the absorptivity as a function of the CN^- equivalents, it must be a 1:1 species with a dissociation constant smaller than 10^{-4}. So the starting compound, after mixing the solutions in the stopped-flow instrument, is the fully formed $[Ni(CN)L]^+$ species. To explain the kinetics results we, therefore, propose the reaction sequence of *Eqns. 1–3*.

$$[NiL]^{2+} + CN^- \overset{K_1}{\rightleftharpoons} [Ni(CN)L]^+; \quad \text{fully formed} \tag{1}$$

$$[Ni(CN)_2L]^+ + CN^- \overset{K_2}{\rightleftharpoons} [Ni(CN)_2L]; \quad K_2 = \frac{[[Ni(CN)L]^+][CN^-]}{[[Ni(CN)_2L]]} \tag{2}$$

$$[Ni(CN)_2L] + CN^- \xrightarrow{k_3} \text{Products} \tag{3}$$

With this model, the CN^- dependencies (*Fig. 1,b*) could be fit but not the pH profile (*Fig. 1,a*). To get a reasonable fit, we had to include a further reaction (*Eqn. 4*) in which HCN is also a reactive species. That HCN can react in such a process is not new, since its reactivity was previously observed with open-chain polyamine Ni^{2+} complexes by *Kolski* and *Margerum* [10]. Assuming that the first equilibrium (*Eqn. 1*) is fully on the product side at the CN^- concentrations we use ($[CN^-]_{tot} > 10^{-3}$ M), one obtains *Eqn. 5* for the rate of the CN^--induced demetallation of $[Ni(\mathbf{1})]^{2+}$. Using pK_{HCN} 9.14 [11], we were able to fit the CN^- dependencies at pH 8.20 and 10.65 as well as the pH dependency. The nonlinear least-squares treatment of all data at once allows one to determine values for the three parameters k_3, k'_3, and K_2. The values are given in *Table 1*, and the quality of the fit is shown in *Fig. 1,a* and *b*.

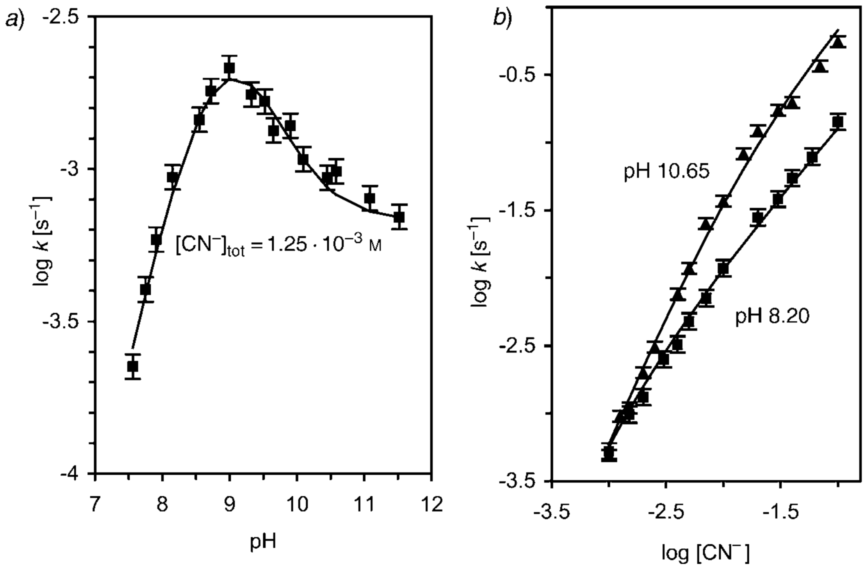

Fig. 1. *Rate of demetallation of* $[Ni(\mathbf{1})]^{2+}$*:* a) *pH profile at* $[CN^-]_{tot} = 1.25 \cdot 10^{-3}$ M *and* b) CN^- *dependencies at pH 10.65 and pH 8.20*

Table 1. *Equilibrium and Rate Constants Obtained by Fitting the Kinetic Data of the Demetallation of the Macrocyclic* Ni^{2+} *Complexes with* **1**–**4** (25°, $I = 0.2$ M (KCl))

	K_1	K_2	k_2	k_{-2}/k_3	k_3	k'_3/k_3
$[Ni(\mathbf{1})]^{2+}$	$< 10^{-4}$	$1.2(1) \cdot 10^{-3}$			1.1(1)	7.8
$[Ni(\mathbf{2})]^{2+}$	$1.8(1) \cdot 10^{-3}$	slow	$4.3(2) \cdot 10^2$	$1.6(1) \cdot 10^{-3}$	*ca.* $2 \cdot 10^{2}$ [a])	4.0
$[Ni(\mathbf{3})]^{2+}$	$1.6(1) \cdot 10^{-2}$	n.o.			$2.0(2) \cdot 10^{3}$ [b])	0.03
$[Ni(\mathbf{4})]^{2+}$	$6 \cdot 10^{-5}$ [c])	$5.2(3) \cdot 10^{-4}$			$1.0(1) \cdot 10^{2}$ [d])	n.o.

[a]) Evaluated assuming $K_2 \sim 10^{-3}$. [b]) Value for $[Ni(CN)L]^+$. [c]) [9]. [d]) Value for *cis*-$[Ni(CN)_2L]$.

$$[Ni(CN)_2L] + HCN \xrightarrow{k'_3} \text{Products} \tag{4}$$

$$v = \frac{[CN^-]}{K_2 + [CN^-]} \cdot \left(k_3[CN^-] + k'_3[HCN]\right)[NiL]_{tot} \tag{5}$$

Nickel(II) Complex of 1,5,8,12-Tetraazabicyclo[10.2.2]hexadecane (**3**). In the case of the Ni^{2+} complex with **3**, the kinetics of the demetallation show a quadratic dependency in $[CN^-]$ at low cyanide and a linear one at higher cyanide concentrations (*Fig. 2,b*). The pH dependences are quadratic in $1/[H^+]$ at low pH and level off at higher pH values (*Fig. 2,a*).

The question of which species is present after mixing the macrocyclic complex and the cyanide solutions was studied at higher $[Ni(\mathbf{3})]^{2+}$ concentrations with 1–5 equiv. of CN^-. The stopped-flow photodiode-array measurements show that the typical band of $[Ni(\mathbf{3})]^{2+}$ at 467 nm (165 M^{-1} cm^{-1}) decreases at a rate too fast to be measured, to give a new species with bands at 328 and 542 nm. The system is clearly in an equilibrium state

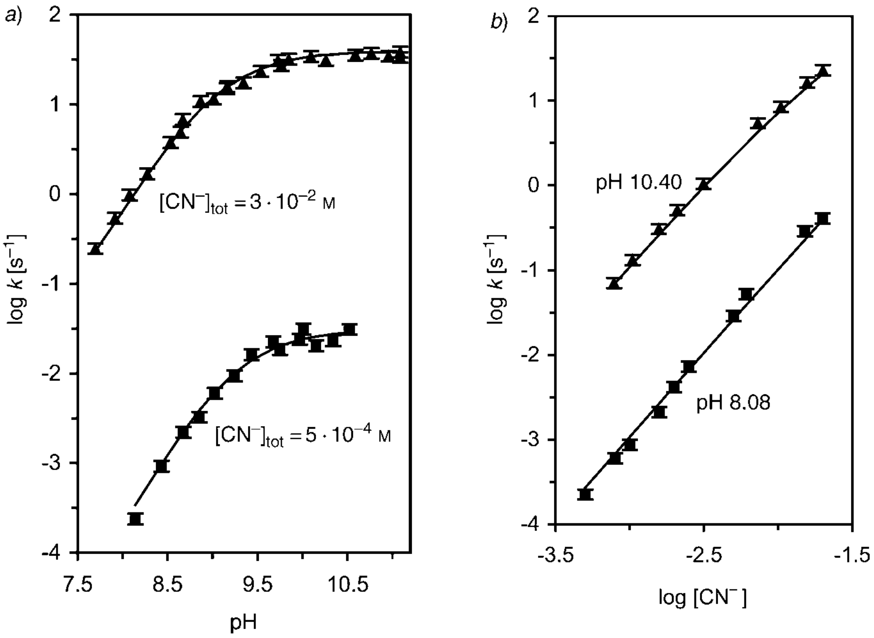

Fig. 2. *Rate of demetallation of [Ni(***3***)]$^{2+}$:* a) *pH profiles at* $[CN^-]_{tot} = 3 \cdot 10^{-2}$ M *and* $[CN^-]_{tot} = 5 \cdot 10^{-4}$ M, *and* b) CN^- *dependencies at pH 10.40 and pH 8.08*

in the range $[CN^-] = 2.5 \cdot 10^{-3}$ M to $1.25 \cdot 10^{-2}$ M. From these observations, we propose the reaction scheme of *Eqns. 6–8*, in which a rapid preequilibrium gives the 1:1 adduct $[Ni(CN)L]^+$, followed by the reaction of it with CN^- or HCN. From this scheme, one obtains the rate law of *Eqn. 9*, with which the three parameters k_3, k'_3, and K_1 can be obtained by a nonlinear least square fitting of the experimental data. Again, pK_{HCN} 9.14 [11] was used for the acid dissociation constant of HCN. The results are given in *Table 1* and the quality of the fit is shown in *Fig. 2,a* and *b*.

$$[NiL]^{2+} + CN^- \overset{K_1}{\rightleftharpoons} [Ni(CN)L]^+; \quad K_1 = \frac{[[NiL]^{2+}][CN^-]}{[[Ni(CN)L]^+]} \tag{6}$$

$$[Ni(CN)L]^+ + CN^- \xrightarrow{k_3} \text{Products} \tag{7}$$

$$[Ni(CN)L]^+ + HCN \xrightarrow{k'_3} \text{Products} \tag{8}$$

$$v = \frac{[CN^-]}{K_1 + [CN^-]} \cdot \left(k_3[CN^-] + k'_3[HCN]\right)[NiL]_{tot} \tag{9}$$

Nickel(II) Complex of 12,12-Dimethyl-1,4,7,10-tetraazacyclotridecane (**2**). If one mixes the Ni^{2+} complex of **2** with 1–5 equiv. of CN^- ions, one can observe that, in a first fast reaction, a 1:1 cyano adduct is formed, which then reacts to a 1:2 species with a rate constant of *ca.* 500 $\text{M}^{-1}\,\text{s}^{-1}$. This value cannot be determined accurately since only relatively small changes in the VIS part of the spectrum take place, and the noise is relatively high.

The demetallation of $[\text{Ni}(\mathbf{2})]^{2+}$ with a large excess of CN^- exhibits a rate with up to a third-order cyanide dependency (*Fig. 3,b*) and shows a 'normal' pH profile with a plateau above pH 10 (*Fig. 3,a*). To fit all data in the VIS and the demetallation with excess of cyanide, we, thus, propose the sequence of *Eqns. 10–13*. From this sequence, the rate law of *Eqn. 14* can be derived applying a steady-state approximation for $[\text{Ni(CN)}_2\text{L}]$. The parameters k_2, k_{-2}/k_3, k'_3/k_3, and K_1 were obtained by a nonlinear least-squares fit of the three pH profiles and the cyanide dependencies with $\text{p}K_{\text{HCN}}$ 9.14 [11]. The values are given in *Table 1*, and the quality of the fit is shown in *Fig. 3,a* and *b*.

$$[\text{NiL}]^{2+} + \text{CN}^- \overset{\text{fast}}{\rightleftharpoons} [\text{Ni(CN)L}]^+; \quad K_1 = \frac{[[\text{NiL}]^{2+}][\text{CN}^-]}{[[\text{Ni(CN)L}]^+]} \tag{10}$$

$$[\text{Ni(CN)L}]^+ + \text{CN}^- \underset{k_{-2}}{\overset{k_{+2}}{\rightleftharpoons}} [\text{Ni(CN)}_2\text{L}] \tag{11}$$

$$[\text{Ni(CN)}_2\text{L}]^+ + \text{CN}^- \xrightarrow{k_3} \text{Products} \tag{12}$$

$$[\text{Ni(CN)}_2\text{L}] + \text{HCN} \xrightarrow{k'_3} \text{Products} \tag{13}$$

$$v = \frac{[\text{CN}^-]}{K_1 + [\text{CN}^-]} \cdot \frac{k_2\left(k_3[\text{CN}^-] + k'_3[\text{HCN}]\right) \cdot [\text{NiL}]_{\text{tot}} \cdot [\text{CN}^-]}{\left(k_{-2} + k_3[\text{CN}^-] + k'_3[\text{HCN}]\right)} \tag{14}$$

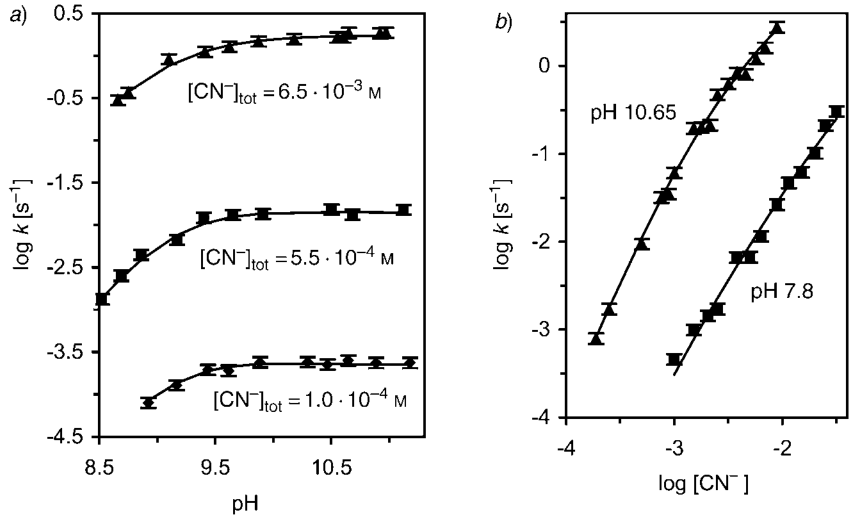

Fig. 3. *Rate of demetallation of* $[\text{Ni}(\mathbf{2})]^{2+}$: a) *pH profiles at* $[\text{CN}^-]_{tot} = 6.5 \cdot 10^{-3}$ M, $[\text{CN}^-]_{tot} = 5.5 \cdot 10^{-4}$ M, *and* $[\text{CN}^-]_{tot} = 1 \cdot 10^{-4}$ M; b) CN^- *dependencies at pH 10.65 and pH 7.80*

Nickel(II) Complex of 1,4,8,11-Tetraazacyclotetradecane (**4**). The preequilibria between $[Ni(\mathbf{4})]^{2+}$ and CN^- have been studied before. *Hinz* and *Margerum* [3] report a 1:1 adduct with $\log K_1 = 4.26$ which was confirmed by our measurements ($\log K_1 = 4.29$ [9]). In addition, one finds also a 1:2 species with spectral properties very similar to those of the 1:1 complex. In the case of $[Ni(\mathbf{4})]^{2+}$, it is expected that the 1:2 complex has a *trans*-structure with the four N-atoms of the macrocycle in the equatorial positions, and the two CN^- axially coordinated.

In contrast to all the other systems here studied, for which the rate of demetallation increases when $[CN^-]$ increases, we observe that at $[CN^-] > 10^{-2}$ M, an inhibition by cyanide takes place (*Fig. 4,b*). So the 1:2 species with *trans*-structure must be unreactive, whereas the 1:1 complex is the species through which the demetallation process takes place. Interesting is that, in this pathway, the reactivity is also dependent on $[OH^-]$ (*Fig. 4,a*). To explain all these observations, we propose the sequence of *Eqns. 15–20*, whereby *trans*-$[Ni(CN)L]^+$ and *cis*-$[Ni(CN)L]^+$ are the *trans*- and *cis*-monocyano-monoaquo species, respectively. Using a steady-state approach for [*cis*-$[Ni(CN)L]^+$] and [*cis*-$[Ni(CN)_2L]$], we obtain for the demetallation rate *Eqn. 21*, from which the parameters k_1, k'_1, k'_{-1}/k'_1, k_2/k_{-1}, k_{-2}, k_3, and K_2 can be obtained from the experimental points. The nonlinear least-squares fit gave $k_1 = 1.2$ (1) M^{-1} s^{-1}, $k'_1 = 1.1$ (1) $\cdot 10^{-4}$ M^{-1} s^{-1}, $k'_{-1}/k_{-1} = 1.4$ (1) $\cdot 10^{-4}$, $k_2/k_{-1} = 10$ (1), $k_{-2} = 33$ (2) s^{-1}, $k_3 = 1.0$ (1) $\cdot 10^2$ M^{-1} s^{-1}, and $K_2 = 5.2$ (3) $\cdot 10^{-4}$ M^{-1}. Some of the results are also given in *Table 1*, and the quality of the fit is shown in *Fig. 4,a* and *b*.

$$[\mathrm{NiL}]^{2+} + \mathrm{CN}^- \overset{K_1}{\rightleftharpoons} \textit{trans}\text{-}[\mathrm{Ni(CN)L}]^+; \quad K_1 = \frac{[[\mathrm{NiL}]^{2+}][\mathrm{CN}^-]}{[\textit{trans}\text{-}[\mathrm{Ni(CN)L}]^+]} \tag{15}$$

$$\textit{trans}\text{-}[\mathrm{Ni(CN)L}]^+ + \mathrm{CN}^- \overset{K_2}{\rightleftharpoons} \textit{trans}\text{-}[\mathrm{Ni(CN)_2L}];$$

$$K_2 = \frac{[\textit{trans}\text{-}[\mathrm{Ni(CN)L}]^+][\mathrm{CN}^-]}{[\textit{trans}\text{-}[\mathrm{Ni(CN)_2L}]]} \tag{16}$$

$$\textit{trans}\text{-}[\mathrm{Ni(CN)L}]^+ + \mathrm{OH}^- \underset{k_{-1}}{\overset{k_1}{\rightleftharpoons}} \textit{cis}\text{-}[\mathrm{Ni(CN)L}]^+ + \mathrm{OH}^- \tag{17}$$

$$\textit{trans}\text{-}[\mathrm{Ni(CN)L}]^+ + \mathrm{H_2O} \underset{k'_{-1}}{\overset{k'_1}{\rightleftharpoons}} \textit{cis}\text{-}[\mathrm{Ni(CN)L}]^+ + \mathrm{H_2O} \tag{18}$$

$$\textit{cis}\text{-}[\mathrm{Ni(CN)L}]^+ + \mathrm{CN}^- \underset{k_{-2}}{\overset{k_2}{\rightleftharpoons}} \textit{cis}\text{-}[\mathrm{Ni(CN)_2L}] \tag{19}$$

$$\textit{cis}\text{-}[\mathrm{Ni(CN)_2L}] + \mathrm{CN}^- \xrightarrow{k_3} \text{Products} \tag{20}$$

$$v = \frac{k_2 k_3 (k'_1 + k_1[\mathrm{OH}^-]) \cdot [\mathrm{NiL}]_{\mathrm{tot}} \cdot [\mathrm{CN}^-]^2}{\left(1 + \frac{[\mathrm{CN}^-]}{K_2}\right)[(k'_{-1} + k_{-1}[\mathrm{OH}^-]) \cdot (k_{-2} + k_3[\mathrm{CN}^-]) + k_2 k_3 [\mathrm{CN}^-]^2]} \tag{21}$$

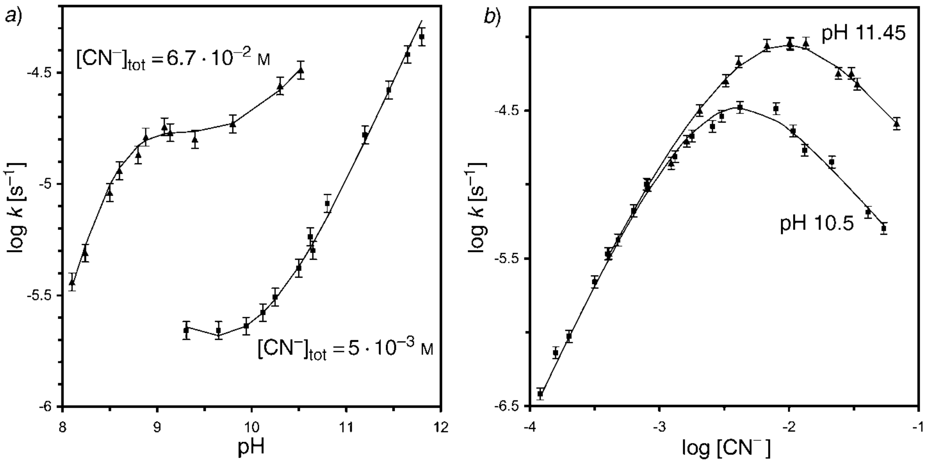

Fig. 4. *Rate of demetallation of [Ni(**4**)]$^{2+}$:* a) *pH profiles at $[CN^-]_{tot} = 6.7 \cdot 10^{-2}$* M *and $[CN^-]_{tot} = 5 \cdot 10^{-3}$* M and b) *$CN^-$ dependencies at pH 11.45 and pH 10.5*

Discussion. – *Preequilibria.* The demetallation of the Ni^{2+} complexes with the macrocyclic ligands **1**–**4** having different ring sizes (from 12 to 14) and including steric factors proceeds in such a way that the first cyano adducts with 1:1 and 1:2 stoichiometry are formed in a relatively rapid reaction, and then these cyano adducts react with further CN^- ions or HCN to give the final products, *i.e.*, $[Ni(CN)_4]^{2-}$ and the free ligand. In this, the macrocyclic Ni^{2+} complexes resemble their analogous complexes with open-chain tetramines [10]. However, when one looks into the details of the reactivity of these macrocyclic Ni^{2+} complexes towards CN^- ions, one finds large differences. For one, the rates encompass almost five orders of magnitude when compared to each other under fixed experimental conditions (pH 10.5, $[CN^-] = 10^{-2}$ M). The slowest to react is [Ni(**4**)]$^{2+}$, the fastest is [Ni(**3**)]$^{2+}$, both systems having a 14-membered macrocycle but different steric factors. As previously described, steric hindrance has drastic effects on the reactivity against CN^-. For example, the square-planar form of the Ni^{2+} complex with 1,4,8,11-tetramethyl-1,4,8,11-tetraazacyclotetradecane, which again has a 14-membered ring, is practically inert towards CN^- at room temperature [9], whereas the square pyramidal form reacts with CN^- at a measurable rate [12]. Of course, the ring size and the steric factors in the reinforced macrocycle have already important consequences for the structure of the starting compounds $[NiL]^{2+}$ as well as for the formation of the cyano adducts $[Ni(CN)_nL]$, which are rapidly formed when $[NiL]^{2+}$ and CN^- solutions are mixed in the stopped-flow instrument.

The twelve-membered macrocycle **1** is clearly too small to encapsulate the Ni^{2+} ion. For the high-spin Ni^{2+} complex, pseudo-octahedral geometry is expected with a folded macrocycle occupying four coordination sites and leaving two *cis*-positions free for unidentate ligands [13] such as CN^- ions to form a 1:2 adduct. Indeed, addition of cyanide gives in two equilibria first the $[Ni(CN)L]^+$ species, which can be observed by a change in the spectral properties as soon as the two components are mixed (*Table 2*), then the $[Ni(CN)_2L]$ complex, which is the reactive species for the demetallation process. In contrast, the 13- and 14-membered macrocycles **2**–**4** give Ni^{2+} complexes

Table 2. *Spectral Properties of the Complexes* $[NiL]^{2+}$, $[Ni(CN)L]^{+}$, *and* $[Ni(CN)_2L]$ *with* L = **1**–**4** (λ_{max} in nm, ε in $M^{-1}\,cm^{-1}$)

	$[NiL]^{2+}$	$[Ni(CN)L]^{+}$	$[Ni(CN)_2L]$
1	560 (10), 356 (17)[b])	780 (7), 510 (10)[b])	
2	428 (100)[a])	810(10), 541 (17), 372 (26)[a])	562 (17), 370 (170)[a])
3	467 (165)[a])	900 (6), 542 (53), 328 (134)[a])	n.o.
4	455 (44.6)[a])	727 (12), 488 (22), 339 (24)[a])[c])	727 (8), 496 (14), 330 (37)[a])[c])

[a]) From experiments with the photodiode array stopped flow. [b]) [9]. [c]) *trans*.

which all show the typical band at 428–465 nm for low-spin square planar coordination geometry (*Table 2*). *Sabatini* and *Fabbrizzi* [14] have, however, shown that, in many cases, there is an equilibrium between the low-spin square-planar form and a hexacoordinated high-spin form in which two molecules of the solvent are involved in coordination. So, here too, it is possible to bind two cyanide ions.

There are, however, distinct differencies between the three systems **2**–**4**. So the $[Ni(\mathbf{2})]^{2+}$ complex has a square-planar coordination geometry with short Ni–N bonds, which indicate that the low-spin metal ion is compressed [15]. It is expected that, when cyanide ions bind to it, a high-spin form results, and the metal ion cannot fit any more into the 13-membered ring. In the case of $Ni(\mathbf{4})^{2+}$, the low-spin Ni^{2+} is perfectly situated in the center of the macrocycle with normal Ni–N bonds. The two *trans* positions are available for unidentate ligands. For the dicyano adduct, a symmetric *trans*-structure will probably result, similar to that found for $[Ni(\mathbf{4})]Cl_2$ [16]. Finally the reinforced Ni^{2+} complex $[Ni(\mathbf{3})]^{2+}$ also has a low-spin square-planar geometry. It has been postulated that the reduced ligand flexibility is responsible for the compression of the hole size, in which low-spin Ni^{2+} still fits, but which cannot adapt to bind the larger high-spin Ni^{2+} ion [17]. With the addition of CN^-, a 1:1 species is formed with characteristic properties of a pentacoordinate high-spin complex. The spectral properties of the starting compounds as well as those of the cyano adducts are collected in *Table 2*.

Mechanism of the Demetallation. The mechanism of the demetallation of the macrocyclic Ni^{2+} complexes by CN^- seems to be different for each of the systems here studied. This is a direct consequence of the structure and properties of the starting compound, which were discussed above.

For **1**, we have the rapid formation of 1:1 and 1:2 cyano adducts to give a complex with a folded macrocycle and a *cis*-octahedral geometry. The geometric situation is, thus, especially favorable for the removal of the macrocycle when additional CN^- or HCN react with it. In a way, this system reminds the situation encountered in Ni^{2+} complexes of open-chain tetramines [10], and it is, therefore, not surprising that the demetallation occurs very rapidly.

The demetallation is clearly more difficult for Ni^{2+} complexes with square-planar structures since it is, expected that dicyano adducts with *trans*-octahedral geometry are formed. The question is, then, how can a metal ion encircled by a macrocycle with the two *trans* positions blocked by CN^- coming out of the ring? Folding of the macrocycle becomes difficult and needs to overcome a high energy barrier, and sliding the macrocycle over the Ni–CN bond seems unrealistic. So, other mechanistic pathways must occur for the demetallation process.

Of the square-planar complexes, the $[Ni(\mathbf{3})]^{2+}$ system is the simplest to understand. It forms only a 1:1 cyano adduct, the formation of the 1:2 species being prevented by the steric interaction of the additional ethylene bridge and by the low flexibility of the ligand to adapt to the large high-spin Ni^{2+} ion. In the 1:1 species, the Ni^{2+} probably comes out of the macrocycle, so that the attack of an additional cyanide ion can come from the same side at which the first cyanide is already bound and can push away the macrocycle from the metal ion. Interesting is that this system is the fastest one to react, although the starting compound has properties very similar to those of $[Ni(\mathbf{4})]^{2+}$, which, on the other side, is the slowest one.

Also relatively fast is the $Ni(\mathbf{2})^{2+}$ system. As discussed above, the Ni^{2+} is compressed in the 13-membered ring so that the low-spin Ni^{2+} hardly fits. In contrast to the other systems here studied, in which the formation of the cyano adducts are rapid preequilibria, we had to introduce rate constants for the forward (k_2) and back reaction (k_{-2}) of the 1:2 adduct formation to fit the experimental data. This observation could indicate that the addition of the second CN^- is a complicated process in which a change of the conformation of the macrocycle probably also takes place. For example, one could think that, with the addition of the second CN^- ion, the macrocycle could fold to give a *cis* 1:2 adduct as the reacting species.

The $[Ni(\mathbf{4})]^{2+}$ complex shows a completely different mechanism from all the other systems. After two rapid preequilibria, the *trans* cyano adduct (*trans*-$[Ni(CN)_2L]$) is formed, but as expected, this species is not reactive. The reactive species, in this case, is the *trans*-cyano-aqua complex, which interconverts to the *cis*-compound (*cis*-$[Ni(CN)L]^+$) by base-catalyzed (H_2O or OH^-) N-inversion of the macrocycle. Such base-catalyzed N-inversions have been observed in the isomerization of macrocyclic Ni^{2+} complexes before [18]. Through the N-inversion, the macrocycle can now fold to give a 1:2 cyano adduct with *cis*-octahedral geometry (*cis*-$[Ni(CN)_2L]$), which then can further react with additional cyanide. Depending on the cyanide concentration, the inversion or the demetallation becomes rate-determining. This gives somewhat strange pH dependencies (*Fig. 4,b*), which, however, are nicely fitted with our model.

The Role of HCN. In several cases, it has been observed that beside CN^- also HCN can react with Ni^{2+} complexes in the demetallation process. In fact, HCN can act as a nucleophile attacking the Ni^{2+} ion and deliver at the same time a proton, which can help to displace one amino group from the metal ion through protonation (see the *Scheme*).

Our results show an interesting aspect about the reactivity of HCN compared to that of CN^-. In the case of $[Ni(\mathbf{1})]^{2+}$ and $[Ni(\mathbf{2})]^{2+}$, HCN is more reactive than CN^- by a

Scheme

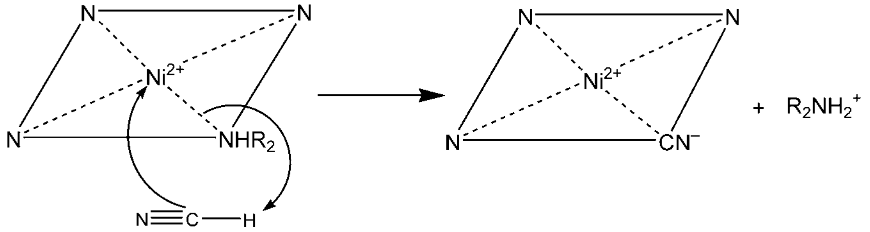

factor of 7.8 and 4.0, respectively. In contrast, no reactivity of HCN is observed for $[Ni(\mathbf{4})]^{2+}$ and only a very small one (factor 0.03) for $Ni(\mathbf{3})^{2+}$. So, only in the two cases, in which the rate-determining step is the displacement of the macrocycle in a folded configuration from a *cis* 1:2 cyano adduct, HCN has an effective chance to react better than CN^-. In the other cases, other factors are responsible for the rate-determining step of the demetallation, and this is probably the cause that HCN cannot compete with CN^-.

In conclusion, we can say that the demetallation of the macrocyclic Ni^{2+} complexes proceeds in such a way that the macrocycle can dissociate from the metal ion, either because the addition of CN^- gives ternary species $[Ni(CN)_nL]$ in which the metal ion is displaced from the center of the ring, or because the ring is in a folded conformation.

This work was supported by the *Swiss National Science Foundation* (Project No 20-66826.01), which is gratefully acknowledged.

Experimental Part

Syntheses. The 1,4,7,10-tetraazacyclododecane (**1**) [19], (12,12-dimethyl-1,4,7,10-tetraazacyclotridecane)-nickel(2+) bis(perchlorate) ($[Ni(\mathbf{2})](ClO_4)_2$) [20], (1,5,8,12-tetraazabiyclo[10.2.2]hexadecane)(nickel(2+) bis(perchlorate)($[[Ni(\mathbf{3})](ClO_4)_2$) [17], (1,4,8,11-tetraazacyclotetradecane)nickel(2+) bis(perchlorate) ($[Ni(\mathbf{4})](ClO_4)_2$) [21] were prepared according to the literature.

The (1,4,7,10-tetraazacyclododecane)nickel(2+) complex $[Ni(\mathbf{1})]^{2+}$ was prepared in soln. by mixing equimolar amounts of $\mathbf{1} \cdot 4$ HCl (0.159 g, 0.5 mmol) and $NiSO_4 \cdot 6\,H_2O$ (0.131 g, 0.5 mmol) in H_2O (20 ml). The mixture was heated for 5 h at 50° and the pH kept at 6–7. Then the volume was adjusted to 50 ml to get a 10^{-2} M stock soln. of $[Ni(\mathbf{1})]^{2+}$.

All measurements were run at $25 \pm 0.1°$ and $I = 0.2$M (KCl).

Kinetics. The CN^--induced dissociation kinetics was followed under pseudo-first-order conditions at 268 nm, where the formation of $[Ni(CN)_4]^{2-}$ can be monitored. Depending on the rate of the reactions, the kinetics were studied using a stopped-flow *Durrum D110* instrument with a 2-cm cell (for **1**–**3**) or a *Varian Techtron-E635* spectrophotometer equipped with a hand stopped-flow setup and a 1-cm cell (**1**, **2**, **4**), or a *Cary 118* spectrophotometer equipped with a sample-changer rack and 1-cm cells (**4**). As buffers, 0.1M 2-[(*tert*-butyl)amino]ethanol (pK_a 11.3), *N*-methylmorpholine (pK_a 8.33), 2-amino-2-methylpropane-1,3-diol (pK_a 9.0) were used. In the case of $[Ni(\mathbf{4})]^{2+}$, NaOH solns. of different concentrations were also used to adjust the pH. Typical concentrations: $[[NiL]^{2+}] = 5 \cdot 10^{-6} - 5 \cdot 10^{-5}$ M, $[CN^-]_{tot} = 10^{-3} - 10^{-1}$ M. The data of the absorbance–time curves were fitted with one exponential function, giving k_{obs} in s^{-1}, from which the bimolecular rates were derived. The different dependencies were calculated in a batch using the Excel solver function [22].

The formation of the different cyano adducts was studied by using a *KinTec Minimixer* stopped-flow instrument with a 2-cm cuvette, connected to a *J&M Tidas-MMS16-VIS500/1* photodiode array with a range of 300–1000 nm. The spectra were recorded with the program *Kinspec235* [23]. Typical concentrations were: $[[NiL]^{2+}] = 2.5 \cdot 10^{-3}$ M, pH 10.5, $[CN^-] = 2.5 \cdot 10^{-3} - 2.5 \cdot 10^{-2}$ M, $I = 0.2$M (KCl). The measurements of the single experiments were fitted with the program *Specifit* [24] to obtain the spectra of the adducts.

REFERENCES

[1] 'Coordination Chemistry of Macrocyclic Compounds', Ed. G. A. Melson, Plenum Press, New York, 1979; L. F. Lindoy, 'The Chemistry of Macrocyclic Ligand Complexes', Cambridge University Press, Cambridge, 1990.

[2] D. K. Cabiness, D. W. Margerum, *J. Am. Chem. Soc.* **1969**, *91*, 6540.

[3] F. P. Hinz, D. W. Margerum, *Inorg. Chem.* **1974**, *13*, 2941.

[4] P. Paoletti, *Pure Appl. Chem.* **1980**, *52*, 2473.

[5] D. K. Cabiness, D. W. Margerum, *J. Am. Chem. Soc.* **1970**, *92*, 2151; B. Bosnich, M. L. Tobe, G. A. Webb, *Inorg. Chem.* **1965**, *4*, 1109.

[6] L. Fabbrizzi, *Commun. Inorg. Chem.* **1985**, *4*, 33.
[7] G. B. Kolski, D. W. Margerum, *Inorg. Chem.* **1968**, *7*, 2239.
[8] N. F. Curtis, *J. Chem. Soc.* **1964**, *2644*; N. Curtis *Coord. Chem. Rev.* **1968**, *3*, 3.
[9] L. Hertli, T. A. Kaden, *Chimia* **1975**, *29*, 304.
[10] G. B. Kolski, D. W. Margerum, *Inorg. Chem.* **1969**, *8*, 1125.
[11] G. Anderegg, *Helv. Chim. Acta* **1957**, *40*, 1022.
[12] M. R. Oberholzer, L. C. Siegfried, T. A. Kaden, *Inorg. Chim. Acta* **1996,** *246*, 41.
[13] M. Ciampolini, M. Micheloni, P. Paoletti, *J. Chem. Soc., Dalton Trans.* **1984**, 1357.
[14] A. Sabatini, L. Fabbrizzi, *Inorg. Chem.* **1979,** *18*, 438.
[15] J. M. Waters, K. R. Whittle, *J. Inorg. Nucl. Chem.* **1972,** *34*, 155.
[16] B. Bosnich, R. Mason, P. Pauling, G. B. Robinson, M. L. Tobe, *J. Chem. Soc., Chem. Commun.* **1965**, 97.
[17] K. P. Wainwright, *Inorg. Chem.* **1980**, *19*, 1396.
[18] P. J. Conolly, E. J. Billo, *Inorg. Chem.* **1987**, *26*, 3224; R. W. Hay, Y. Q. Chen, *Inorg. Chim. Acta* **1991**, *180*, 147.
[19] E. J. Richman, T. J. Atkins, *J. Am. Chem. Soc.* **1974**, *96*, 2268.
[20] N. F. Curtis, G. W. Prader, *J. Chem. Soc.* **1971**, 1771.
[21] E. K. Barefield, F. Wagner, A. D. Herlinger, A. R. Dahl, *Inorg. Synth.* **1976**, *16*, 220.
[22] E. J. Billo, 'Excel for Chemists', Wiley-VCH, NewYork, 2001.
[23] K. D. Karlin, N. Wei, B. Jung, S. Kaderli, P. Niklaus, A. D. Zuberbühler, *J. Am. Chem. Soc.* **1993**, *115*, 9506.
[24] H. Gampp, M. Mäder, Ch. J. Meyer, A. D. Zuberbühler, *Talanta* **1985**, *32*, 257; R. Binstead, A. D. Zuberbühler, to *Spectrum Software Associates* (Chapel Hill, NC), *Specfit/32*®, Copyright 2000–2002.

Received July 2, 2004